

Operating limits study based on Finite Elements of a Brushless Doubly-fed Induction Machine

Idhir Nezzari *, Kessal Abdelhalim †

Abstract

The Brushless Doubly-fed Induction Machine (BDFIM) is a new topology machine proposed for the generation of electrical energy at variable speed. The stator of this machine has two independent windings with different numbers of poles (power winding and control winding). Its functioning is conditioned by certain physical constraints, i.e., the relation between the speed of the rotor, the polarities of the two windings and their frequencies. We have developed in this paper a finite element model to study and verify the operating limits of the BDFIM (2.2 Kw and 1/3 pairs of poles) on flux2d.

Keywords: Brushless Doubly-Fed Induction Machine (BDFIM), Variable Speed Generation, Finite Elements, synchronous mode

1 Introduction

The Brushless Doubly-fed Induction Machine (BDFIM) presents a very attractive solution for variable generation: its power winding ('PW') is directly connected to the grid, the control winding ('CW') is supplied by a static converter and its rotor can be cage or nested rotor. This machine combines the advantages of both the cage rotor machine and the wound-rotor machine. The wound-rotor machine is heavier and more cumbersome than its cage equivalent for the same power. Moreover, the absence of brushes in the BDFIM relieves us of frequent maintenance.

Cascade induction machines were the first practical implementation of a doubly fed brushless machine. René and his research group patented a prototype of the BDFIM, proposed in their research [1]. Tim D. Strous presented a study on the development and research defeats of the BDFIM for wind turbines [2]. BDFIM is a promising solution in the field of variable speed electric power generation compared to other types of generators on the market [3]. Thorough study is, however, needed to improve its operation. Wang

Xuezhou developed a finite element model for study and optimization of the machine [4]. Paul C. Roberts devoted a part of his thesis to studying the various types of rotors possibly suited to the machine [5] and Fengge Zhang compared a different structure of rotors and its influence on machine performance in [6]. [7] analyzed a series of pairs of pole pairs for the stator. [8] studied machine performance using finite element modeling. [9] analyzed a 6-2 poles machine using the finite element method. In order to study our machine, we developed a numerical model by the finite element method, using flux2d to test its operating limits. We start with the natural synchronization of the machine. Subsequently, we will proceed to supply the control winding with different frequencies.

2 Operation mode of the BDFIM

The BDFIM comprises a stator composed of two windings, one with power connected directly to the grid and the other to control the magnetic state of the machine, with different numbers of poles p_1 and p_2 respectively.

In the supply mode of the two stators, several modes of operation can be distinguished:

- The BDFIM can be used as an induction machine with either p_1 or p_2 pole pairs, by feeding winding 1 or 2 respectively, and leaving the other winding open.
- If the open stator is short-circuited, the behavior of the machine is similar to a cascaded induction machine with $p_1 + p_2$ pairs of poles.

In dual supply mode, the BDFIM presents a synchronous mode of operation, desirable for electrical generation. This synchronous operation mode of the BDFIM is based on the existence of a cross magnetic coupling between the two stator windings through the rotor [1].

Crossed magnetic coupling is the coupling of the field produced by the power winding (PW) to the field produced by the control winding (CW) across the rotor

*LPMRN Laboratory, Faculty of Sciences & Technology, Bordj Bou Arreridj University [e-mail](#)

†LPMRN Laboratory, Faculty of Sciences & Technology, Bordj Bou Arreridj University [e-mail](#)

and vice versa, This may be possible by choosing the number of poles of each different winding [5], which also avoids the undesirable direct coupling between the two windings.

The magnetic induction created by the two windings in the air gap will take the following form (taking into account only the fundamentals of the magnetic induction):

$$b_c(\theta, t) = B_c \cos(w_c - p_c\theta)$$

$$b_p(\theta, t) = B_p \cos(w_p - p_p\theta)$$

c, p : indicate control and power winding

b : magnetic induction

θ : angular position

w : angular pulsation

If the rotor turns to w_r rad/s, then (1) and (2) can be written in the rotor reference ($\theta' = \theta + w_r t$) as follows:

$$b_c(\theta', t) = B_c \cos((w_c - p_c w_r) t - p_c \theta')$$

$$b_p(\theta', t) = B_p \cos((w_p - p_p w_r) t - p_p \theta')$$

r : indicates the rotor.

Therefore, the magnetic inductions in the reference frame of the rotor are progressive waves of frequency $(w_c - p_c w_r)$ and $(w_p - p_p w_r)$ respectively. The cross-coupling between the two windings of the stator is based on the inability to separate the induced currents in the rotor. So the currents induced by b_c in the rotor couple with b_p and vice-versa. The current induced by the magnetic field will therefore have the same frequency as in the synchronous state. Therefore, if constant torque is produced by the cross coupling then: $(w_c - p_c w_r) \pm (w_p - p_p w_r) = 0$. Taking the negative value:

$$w_r = \frac{w_c + w_p}{p_c + p_p}$$

$$N_r = p_c + p_p$$

N_r : number of rotor nests

Equation (5) gives the rotor speed corresponding to the synchronous operation of the machine. In addition, there must be spatial compatibility for the existence of cross-coupling. This requirement can be satisfied by designing a special rotor.

3 Modeling of the BDFIM by the finite element method

A finite element model has been developed on flux2d software to analyze the behavior of the machine. The prototype parameters are shown in Table 1.

Description	Machine Parameter	Value
-Rated power (KW)	P	2.2
-External radius (mm)	R	134.5
-Width of the air gap(mm)	lg	0.6
-Stator slots	Nss	36
-Height of the stator slot (mm)	hs	12.19
-Pole pairs	p,c	13
-Rotor nests	Nnest	4
-Height of the rotor slot (mm)	hr	27.5

Table 1: Main parameters of the prototype

3.1 Geometry and mesh

Figure 1 shows the geometry of the studied BDFIM, built with Flux 2D.

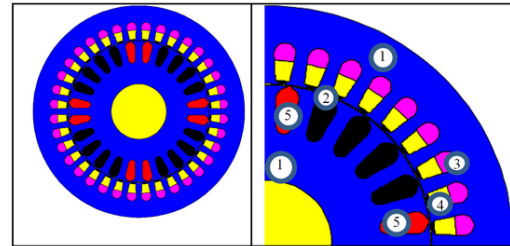
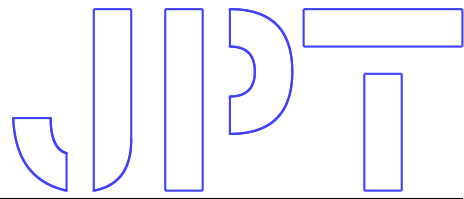


Figure 1: Geometry of the machine under flux2D: (1) Stator and rotor (magnetic core), (2) Air gap, (3) Power winding, (4) Control winding, (5) Rotor nest

This figure represents the various zones of the BDFIM: Iron, air and the conductors. Each area is assigned its electromagnetic properties, the resistivity of conductive materials and the magnetic properties of linear and non-linear materials represented by their saturation curve $B(H)$.

Taking into account the assumptions adopted for the 2D model, the partial differential equation governing the diffusion of the electromagnetic field in the machine is:

$$-\frac{\partial}{\partial x} \left(\frac{1}{\mu} \frac{\partial a}{\partial x} \right) - \frac{\partial}{\partial x} \left(\frac{1}{\mu} \frac{\partial a}{\partial x} \right) = J_s - \sigma \left(\frac{\partial a}{\partial t} + \right) \text{grad}(V)$$



a: potential vector

where:

$$\text{div} \left(\frac{1}{\mu} \text{grad} (a) \right) + \sigma \left(\frac{\partial a}{\partial t} + \partial \text{grad} (v) \right) = -J_s$$

According to Fig. 1 three different regions are distinguished in the study of the BDFIM compared to the second term of the equation (8):

Stator: The conductivity of the stator iron is zero, because it consists of thin sheets insulated from each other. The BDFIM stator contains two windings, which leads to the existence of two current densities imposed by the two supplies of this stator. They are uniformly distributed over the surface of the slot. This gives a vector potential in the stator verifying the following equation: in the iron:

$$i_v \left(\frac{1}{\mu} \text{grad} (a) \right) = 0$$

in the slots:

$$i_v \left(\frac{1}{\mu} \text{grad} (a) \right) = -(J_{s1} + J_{s2})$$

In order to couple these magnetic equations to the electrical circuits of the two windings current densities ($J_{s1} + J_{s2}$) will be expressed according to the phase currents:

$$J_{s1,2} = \frac{n_{e1,2}}{s_{e1,2}} \beta (\alpha_{a1,2} i_{a1,2} + \alpha_{b1,2} i_{b1,2} + \alpha_{c1,2} i_{c1,2})$$

$n_{e1,2}$: Number of winding conductors 1 or 2 per slots

$s_{e1,2}$: Surface of the slot occupied by the $n_{e1,2}$ conductors of winding 1 or 2

β : A coefficient equal to (± 1) giving the direction of conductors and ($\alpha_{a1,2} i_{a1,2} + \alpha_{b1,2} i_{b1,2} + \alpha_{c1,2} i_{c1,2}$) which define which slot belongs in the phases (a 1,2 , b1,2 , c1,2) By replacing the value of $J_{s1,2}$ in (11):

$$\text{div} \left(\frac{1}{\mu} \text{grad} (a) \right) + \begin{cases} \frac{n_{e1}}{s_{e1}} \beta (\alpha_{a1} i_{a1} + \alpha_{b1} i_{b1} + \alpha_{c1} i_{c1}) \\ \frac{n_{e2}}{s_{e2}} \beta (\alpha_{a2} i_{a2} + \alpha_{b2} i_{b2} + \alpha_{c2} i_{c2}) \end{cases}$$

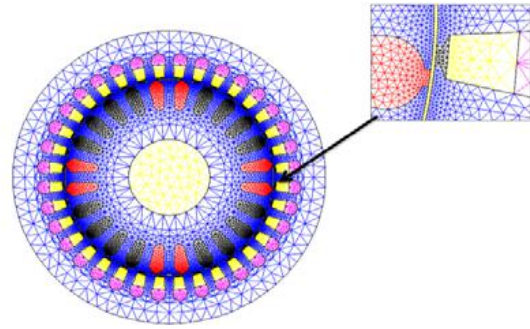


Figure 2: Mesh of the machine

3.2 Simulation results

In this part we report on the several simulation tests we performed to study the machine. Starting with the synchronization test, we connected the power winding directly to the grid and short-circuited the control winding. Then we supplied the control winding with different frequencies (2, 4, 25 Hz 4 and -2, -4, -25 Hz); the power winding was connected to the grid. The frequency and voltage of the PW are set by the grid ($f_p=50\text{Hz}$, $V_{p,max}=311\text{V}$). We considered the machine without load torque and with a viscous coefficient of friction $K_f=0.03 \text{ Kg}\cdot\text{m}^2/\text{s}$ and inertia $J=0.1 \text{ Kg}\cdot\text{m}^2$.

3.3 Synchronization test of the machine:

The rotor speed and electromagnetic torque are shown in Fig. 3 and Fig. 4. After a long transient (6s), the speed of the BDFIM stabilizes, in steady state, at its value of natural synchronism $\Omega_r=750 \text{ rpm}$ (Fig. 3 - vitesse is speed and temps is time).

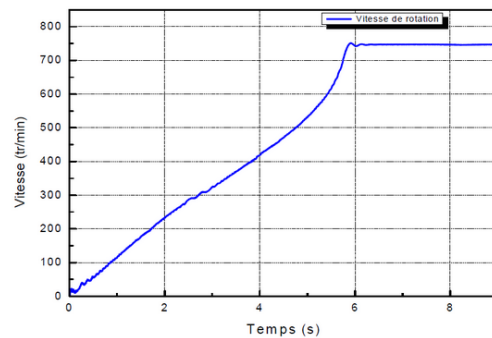


Figure 3: Rotor speed (rpm)

Once the synchronization speed is reached (750 rpm), the frequency and amplitude of the control winding currents corresponding to this synchronous operating

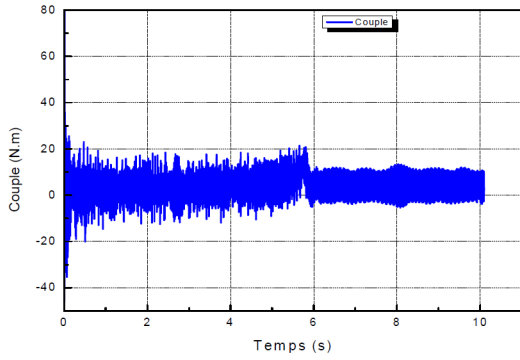
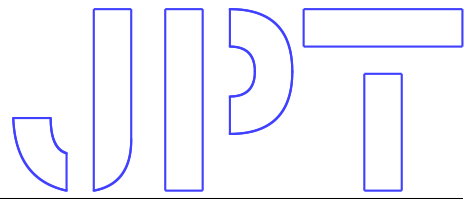


Figure 4: Electromagnetic torque (Nm)

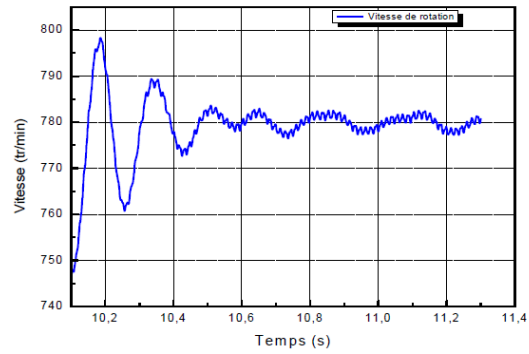


Figure 6: Rotor speed ($f_c = -2 \text{ Hz}$)

mode are practically zero (Fig. 6). This value of f_c checks the synchronization condition in eq. (5).

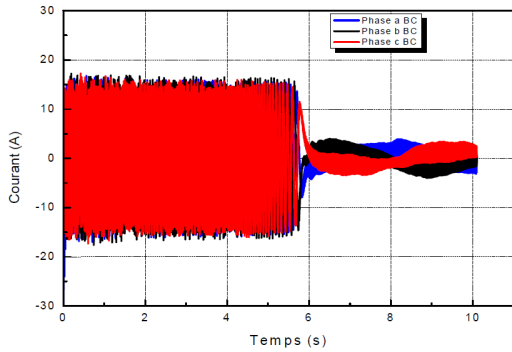


Figure 5: Control winding currents (A)

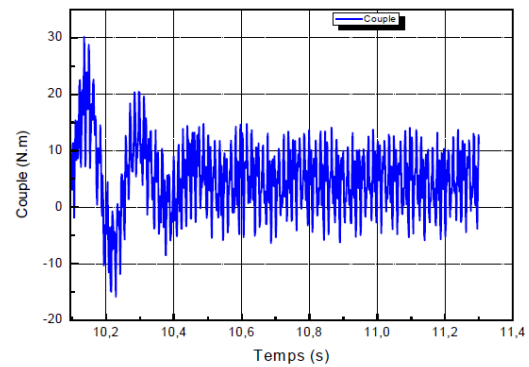


Figure 7: Electromagnetic torque ($f_c = -2 \text{ Hz}$)

3.4 Supplying the control winding with different frequencies

We now focus on use of the frequency of the control winding to vary the speed of the BDFIM. The control winding supplies at different frequencies in one direction then in the opposite direction. In order to ensure sufficient magnetization of the machine, we used the equation: $\frac{V_{c_{max}}}{w_c} = 0.7$ [1].

Positive direction: Once the machine was synchronized, we supplied the CW with: $f_c = 2 \text{ Hz}$ at $t = 10.1 \text{ s}$, then $f_c = 4 \text{ Hz}$ at $t = 11.3 \text{ s}$.

Rotor speed and electromagnetic torque are represented in Fig. 6 and Fig. 7.

We observed that rotor speed, after oscillations, increased to 780 rpm. This corresponds to:

$$\Omega_r(f = 2 \text{ Hz}) = \frac{2\pi \cdot 50 + 2\pi(+2)}{4} \cdot \frac{60}{2\pi} = 780 \text{ rpm}$$

For $f_c = 4 \text{ Hz}$, the speed of the BDFIM increased from 780 rpm to 810 rpm with large fluctuations. This corresponds to:

$$\Omega_r(f = 4 \text{ Hz}) = \frac{2\pi \cdot 50 + 2\pi(+4)}{4} \cdot \frac{60}{2\pi} = 809,7 \text{ rpm}$$

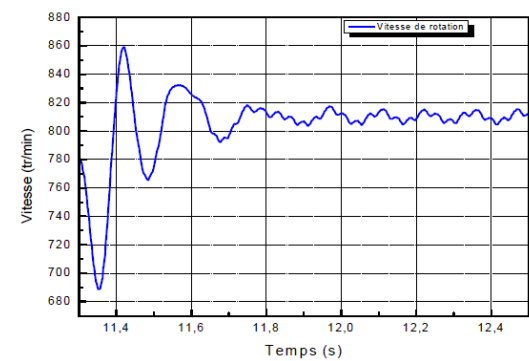


Figure 8: Rotor speed ($f_c = 4 \text{ Hz}$)

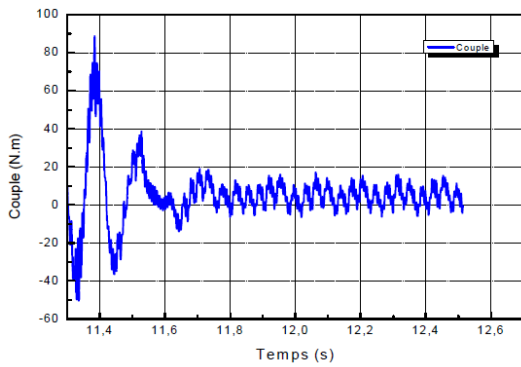


Figure 9: Electromagnetic torque ($f_c=4Hz$)

Second Direction: Once the machine is synchronized we supply the control winding CW with $f_c=-2Hz$ then $f_c=-4Hz$. The results obtained are shown in Fig. 10 and Fig. 11.

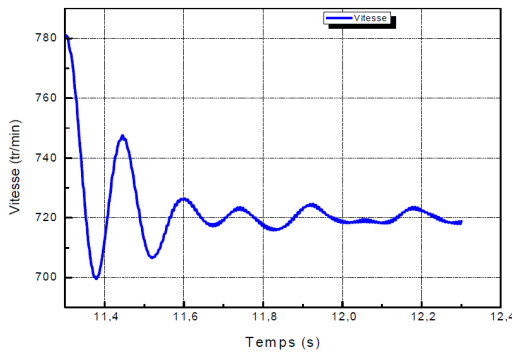


Figure 10: Rotor speed ($f_c=-2Hz$)

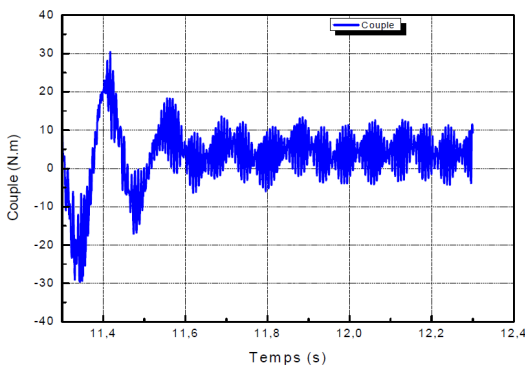


Figure 11: Electromagnetic torque ($f_c=-2Hz$)

It is clear that the speed of the BDFIM, after oscillations, falls to 720 rpm. This corresponds:

$$\Omega_r(f = -2 Hz) = \frac{2\pi \cdot 50 + 2\pi(-2)}{4} \cdot \frac{60}{2\pi} = 719.7 rpm$$

For frequency $f_c=-4Hz$, applied at $t = 12.3s$, the results obtained are shown in Fig. 12 and Fig. 13.

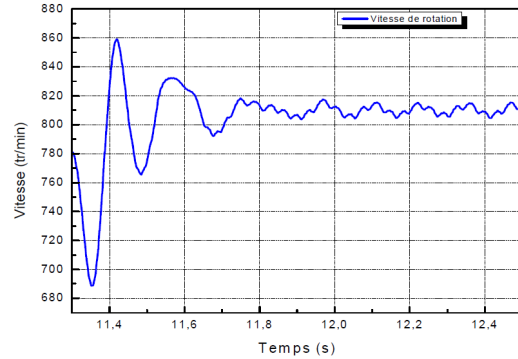


Figure 12: Rotor speed ($f_c=-4Hz$)

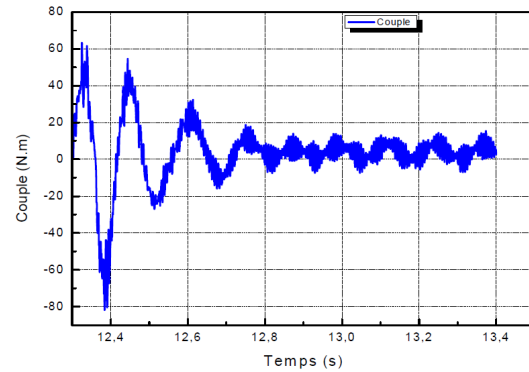


Figure 13: Electromagnetic torque ($f_c=-4Hz$)

For this frequency the speed continued to decrease, falling from 720 rpm to 690 rpm with fluctuations. This corresponds to:

$$\Omega_r(f = -4 Hz) = \frac{2\pi \cdot 50 + 2\pi(-4)}{4} \cdot \frac{60}{2\pi} = 689.7 rpm$$

The results obtained confirm eq. ??.

We now consider control winding frequencies up to $f_c = 20Hz$ and $-25Hz$ to determine the operating limits of our machine.

The results of simulations obtained show the operating instability of the BDFIM for $f_c = 20Hz$. In fact, the speed and torque are very wavy (see Fig. 14 and Fig. 15). The speed oscillates between 699 and 770rpm and torque between -60 and $90N.m$.

The BC was fed at frequency $f_c = -25Hz$ and voltage $V_{(c,eff)} = 77.75v$. The results obtained in Fig. 16 and Fig. 17 show the same observations as made previously.

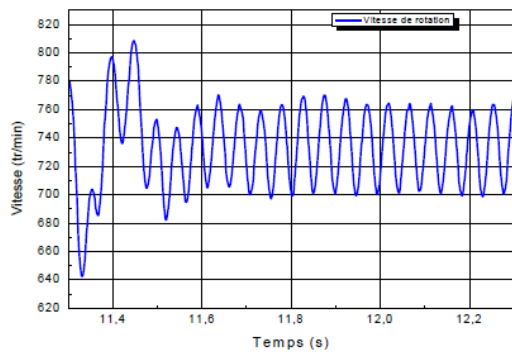


Figure 14: Rotor Speed ($f_c=20\text{Hz}$)

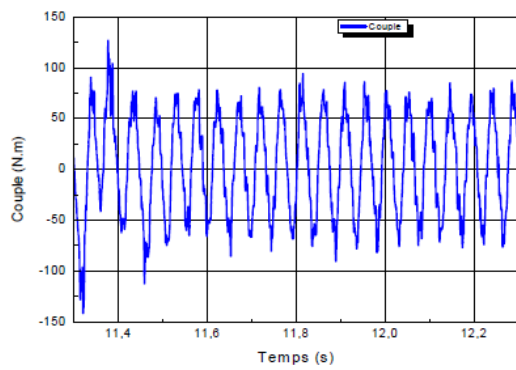


Figure 15: Electromagnetic torque ($f_c=20\text{Hz}$)

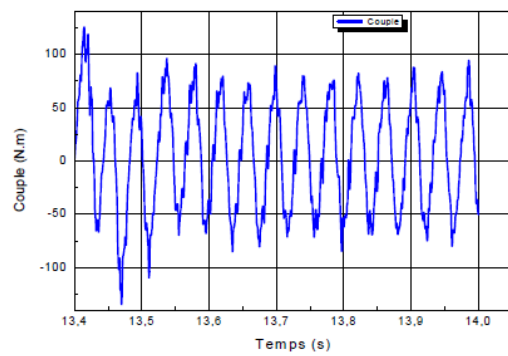


Figure 17: Electromagnetic torque ($f_c=-25\text{Hz}$)

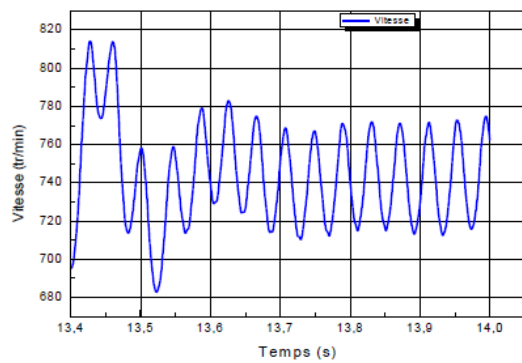


Figure 16: Rotor speed ($f_c=-25\text{Hz}$)

4 Conclusion

The finite element model developed was very useful for studying the functioning limits of the BDFIM. With this model we have solved the magnetic problem, electrical circuits, and mechanical movement step by step in time using flux2d.

The study carried out in this paper allowed us to verify the physical operating constraints of the BDFIM, i.e., the natural synchronization and the law of variation of speed as a function of the frequency of the control winding.

The synchronization test showed that the currents induced in the control winding had the same frequencies as calculated analytically, and as the frequency increases the speed always follows the synchronization condition. However, once we arrive at limit frequencies $f_c = 20\text{Hz}$ or $f_c = -25\text{Hz}$ we note a deterioration in the performances of the BDFIM.

This paper gives us an overview for understanding BDFIM behavior and the constraints of its functioning. However, future work needs to focus on optimization in order to market the machine, designing a special structure dedicated to the doubly-fed application instead of making modifications to conventional asynchronous machines.

References

- 1.Lobo, P. (2003) Modélisation, Conception et Commande d'une Machine Asynchrone sans Balais Doublement Alimentée pour la Génération à Vitesse Variable.
- 2.Strauss, T.D. (2016) Brushless doubly-fed induction machines for wind turbines: developments and research challenges. *IET Journals*, **11**.
- 3.Strous, T.D., Shipurkar, U., Polinder, H., and Ferreira, J.A. (2016) Comparing the Brushless DFIM to other Generator Systems for Wind Turbine Drive-Trains. *Journal of Physics: Conference Series*, **753**, 112014.
- 4.Wang, xuezhou (2017) Modeling and Design of Brushless Doubly-Fed Induction Machines.
- 5.Robbert, P.C. (2005) A Study of Brushless Doubly-Fed (Induction) Machines.
- 6.Zhang, F., Yu, S., Wang, Y., Jin, S., and Jovanovic, M.G. (2019) Design and Performance Comparisons of Brushless Doubly Fed Generators With Different Rotor Structures. *IEEE Transactions on Industrial Electronics*, **66** (1), 631–640.

7.Blij, N.H. van der, Strous, T.D., Wang, X., and Polinder, H. (2014) A novel analytical approach and finite element modelling of a BDFIM. *2014 International Conference on Electrical Machines (ICEM)*.

8.I.Nezzari, A.K. (2019) Finite element modeling and performances studying of a BDFIM, case of a machine with 8-4 pairs of poles. *CEE2019, Ecole Militaire Polytechnique, Algeria*.

9.I.Nezzari, A.K. (2019) Finite Element Modeling and Analysis of a 6/2 Poles Brushless Doubly-Fed Induction Machine. *SSD'19, Istanbul, Turkey*.